Surface Characterization of Ni-Mg-Al and Co-Mg-Al Hydrotalcites Investigated by Inverse Gas Chromatography

[1]Zhiyin Sun, [2,4]Guanghua Xia, [1]Wenyuan Tang and [3]Wenchu Wang*
[1]*Taizhou University, Taizhou 318000, P.R.China.*
[2]*Zhejiang University of Technology, Hangzhou 310014, P.R.China.*
[3]*Taizhou Municipal Bureau of Forestry, Taizhou 318000, P.R.China.*
[4]*Taizhou Pollution Control and Engineering Technology Center, Taizhou 318000, P.R.China.*
515198501@qq.com*

(Received on 12th May 2017, accepted in revised form 5th May 2018)

Summary: Carbonate pillared hydrotalcite-like compounds ($Ni_xMg_{3-x}Al$-LDHs and $Co_xMg_{3-x}Al$-LDHs) with different molar ratios were synthesized through co-precipitation, the samples were characterized by XRD, FTIR and Inverse gas chromatography (IGC) techniques. The surface properties were compared and verified by computer simulation. The results indicated that with the increasing of Ni^{2+} in $Ni_xMg_{3-x}Al$-LDHs, the surface adsorption free energy and the dispersive component of the surface energy decreased, while the stability increased gradually, which was contrary to the Co^{2+} in $Co_xMg_{3-x}Al$–LDHs. Besides, the surface free energy of Ni-Mg-Al hydrotalcites was smaller than Co-Mg-Al hydrotalicites when they were in the same molar ratio, and the stability of the former was stronger than the latter.

Keywords: Inverse gas chromatography (IGC); Hydrotalcites; Surface characterization.

Introduction

Layered double hydroxides (abbreviated as LDHs), also known as hydrotalcite-like compounds or anion clays, which are well known for their applications in the filed of catalysts, sorbents, composite additives and ion-exchangers etc [1,2]. Metal hydroxide with divalent and trivalent metal ions, with adjustable degeneration, can form the hydrotalcite with catalytic activity by introducing with transition metal ions, such as Cu^{2+} , Ni^{2+} and Co^{2+} etc [3,4].

Recently, the study of Co^{2+} and Ni^{2+} hydrotalcites concentrated in catalysis and adsorption etc. Zhao et al.[5] synthesized carbon nanotubes by using the calcined product of ternary magnesium nickel aluminum LDHs, the results showed that the catalytic properties is related to the content of nickel. Liu et al. [6] found that with the increase of cobalt content in LDHs, the catalytic activity of isopropanol increased, and the catalytic product selectivity was also associated with the surface properties of hydrotalcite. Zhao et al.[7] had researched benzaldehyde oxidation reaction by grafting Ni-Al-LDHs on carbon nanotubes as catalyst, results showed that Ni-Al-LDHs had good catalytic performance, and the main reason for the higher catalytic efficiency was the improvement of the catalyst dispersion. It's obvious that the surface properties of materials play a decisive role in catalysis and adsorption, which have important reference value for practical application. Considering the research on the surface properties of LDHs with catalytic activity is still very scarce, it's very meaningful to explore the surface properties of Ni-Mg-Al-LDHs and Co-Mg-Al-LDHs.

Inverse gas chromatography (IGC) is one of the most sensitive, reliable, and convenient methods to study the surface properties [8]. This method was first used to study the interaction between polymer and probe molecules, and the compatibility between polymer and polymer. In recent years, some researchers applied this technology in researching the surface properties of kaolin [9], montmorillonite [10] and other inorganic materials and modified materials.

By using this method, our workgroup [11,12] had studied the difference between the surface properties of Mg-Al-LDHs and its modified products, including the Cu-Mg-Al-LDHs' surface properties. In this paper, we applied IGC method to investigate the surface properties of Ni-Mg-Al-LDHs and Co-Mg-Al-LDHs. Simultaneously, the conclusion was validated by studying the stability and Jahn-Teller effect of the two systems with computer simulation [13].

Experimental

*Sample preparation***:** In a typical experiment,

***To whom all correspondence should be addressed.**

$Ni_xMg_{3-x}Al$-LDHs (x=0-3) were synthesized by a modified co-precipitation method [17]. Specifically, an aqueous solution (100 mL) named A was prepared with NaOH (0.2 mol) and Na_2CO_3 (0.025 mol), another aqueous solution (100 mL) named B was prepared with $Ni(NO_3)_2{\cdot}6H_2O$ (0.025 mol), $Mg(NO_3)_2{\cdot}6H_2O$ (0.05 mol) and $Al(NO_3)_3{\cdot}9H_2O$ (0.025 mol), after that, both A and B were added dropwise to a three neck round bottom flask with vigorous stirring, maintain the pH of 9 to 10, then keep stirring 1h. After the reaction, the resulting precipitate was crystallized at 323K for 18 h, and then centrifuged and washed with distilled water for several times and was finally dried in vacuo at 338K for 12 h, giving the product $NiMg_2Al$-LDHs.

The preparation of Ni_2MgAl-LDHs, Ni_3Al-LDHs, Mg_3Al-LDHs, Co_3Al-LDHs, Co_2MgAl-LDHs and $CoMg_2Al$-LDHs were made by changing the mole ratio of Ni, Al and Mg according to the methods described above.

Pentane, n-hexane and n-heptane, octane are made from Sinopharm Chemical ReagentCo., Ltd. And other chemicals were made from JuHua group corporation.

*The instrument and reagent***:** The chromatographic experiments were performed with a GC7890(□) gas chromatograph equipped with thermal conductivity detector (TCD). Retention times were recorded on an N-2000 integrator.

The probes used were n-pentane, n-hexane, n-heptane, and n-octane, all reagents were obtained in the higher purity grade possibly and directly used as received without further purification.

*Characterization***:** Preparation of chromatographic column: A stainless steel column with a length of 15 cm and an internal diameter of 0.2 cm. To prepare packings for IGC, the clays were pressed into pellets using a press at 20 tonne pressure, then crumbled and sieved to give aggregates of 250 µm. Clean it with acetone, leave to dry completely and then fill in with the prepared LDHs materials respectively, after that, all the columns were aged at 443 K under a constant nitrogen flow (30mL/min) for 1h.

IGC analysis: A GC7890(□) gas chromatograph equipped with thermal conductivity detector, with high purity nitrogen (99.99% pure) as the carrier gas at a flow rate of 50 mL/min, which was measured at the detector outlet with soap bubble flowmeter. Both the detector temperature and gasification chamber temperature were set at 453 K, and the column temperature was conditioned by heating at 403-433 K.

X-ray diffraction (XRD) was carried out using a Shimadzu XRD-6000 diffractometer, with Cu-Kα radiation (λ=0.1542 nm) at a scan speed of 5°/min.

Bruker Vector 22 FT-IR spectra in the range 4000 – 400 cm^{-1} was used to analyze the structure of the sample (the mass ratio of the sample to KBr was 1/100).

Results and Discussion

Inverse gas chromatography

*Surface adsorption free energy***:** In this paper, C_5-C_8 straight-chain alkanes as probe molecules, the intermolecular interaction force between molecules is neglected in the infinite dilution region. The relationship between adsorption free energy ΔG^0 and retention volume V_N is described as follows [14,15]:

$$\Delta G^0 = -RT\ln\left(\frac{V_N P_0}{\pi_0 mS}\right) \quad (1)$$

$$V_N = (t_R - t_m)\cdot F_a \cdot \frac{T}{T_a}\cdot J \quad (2)$$

$$J = \frac{3}{2}\left[\frac{(p_i/p_o)^2 - 1}{(p_i/p_o)^3 - 1}\right] \quad (3)$$

where: R is ideal gas constant, where S is the specific surface area of the adsorbent, m the weight of sample in the column, π_0 is the surface pressure of the liquid probe and P_0 the equilibrium vapour pressure of the probe under standard conditions ,t_R and t_m are the retention time and dead times, T is the column temperature, F_a is the flow rate at the end of column at room temperature T_a, J is the James-Martin factor for the correction of gas compressibility, p_o is outlet pressure, and p_i is inlet pressure.

The retention volume V_N was obtained by

testing a series of probe molecules on the Hydrotalcite-Like compounds, and the corresponding surface free energy (ΔG^0) of adsorption were calculated and summarized in

Table-1: ΔG^0 VALUES OF $Ni_xMg_{3-x}Al$-LDHs AND $Co_xMg_{3-x}Al$-LDHs (x=0-3) AT 423 K.

	$-\Delta G^0$/(KJ·mol^{-1})			
System	**n-Pentane**	**n-Hexane**	**n-Heptane**	**n-Octane**
Ni_3Al-LDHs	**10.76**	**7.49**	**-**	**-**
$MgNi_2Al$-LDHs	**14.82**	**11.22**	**8.78**	**7.27**
Mg_2NiAl-LDHs	**16.12**	**12.96**	**11.11**	**8.53**
Mg_3Al-LDHs	**18.34**	**15.58**	**13.54**	**12.47**
Mg_2CoAl-LDHs	**10.97**	**7.80**	**5.35**	**5.35**
$MgCo_2Al$-LDHs	**16.56**	**13.88**	**12.12**	**10.64**
Co_3Al-LDHs	**16.61**	**14.29**	**-**	**-**

As shown in Table 1, the surface adsorption free energy of all LDHs were below zero, indicating that the reaction of n-alkanes adsorbing on the solid surface could be carried out at room temperature spontaneously.

According to the probe arrangements from the above list, n-alkane with more carbon atoms tends to have less surface adsorption free energy, this is due to the increasing of carbon atoms, the alkanes are getting more and more difficult to enter into the LDHs molecule structure or adsorb on it [12].

As we found in the $Ni_xMg_{3-x}Al$-LDHs system, the surface free energy decreased with the increase of Ni^{2+}, and this may be due to the introduction of Ni^{2+} that formed a more stable octahedron, which reduced the adsorption energy. While, as the content of Co^{2+} in the Co/Mg/Al- LDHs systems increasing, a certain degree of distortion may occur in layer board structure, so the surface adsorption free energy increased.

By comparing the surface adsorption free energy of $Ni_xMg_{3-x}Al$-LDHs and $Co_xMg_{3-x}Al$-LDHs, we found the adsorption capacity of Co/Mg/Al-LDHs was larger than Ni/Mg/Al-LDHs if the x were equal, suggesting that LDHs with Co^{2+} possess had more powerful surface activities.

Dispersive component of surface energy

$$\gamma_s^d = \frac{1}{\gamma_{CH_2}} \cdot \left(\frac{\Delta G_{CH_2}}{2 \cdot N \cdot a_{CH_2}}\right)^2 \qquad (4)$$

$$\gamma_{CH_2} = 36.8 + 0.058(293 - T) \qquad (5)$$

where N is Avogadro's number, γCH_2 is the surface energy of a hypothetical substance that contain only methylene groups and αCH_2 is the cross-sectional area of a methylene group (α_{CH2}=0.06 nm^2). Thus, at constant temperature, for a series of alkane probes, a plot $RT\ln V_n$ versus the number of carbon atoms should give a straight line, and then obtained ΔG_{CH2} from the linear slope .

As shown in Fig.1 and Fig.2, the $RT\ln V_n$ of the material show a good linear relationship with the number of carbon number (the linear slope reflects the increment of the adsorption free energy), indicating that $\Delta G CH_2$ is reliable and could be used to calculate γ_s^d at a high confidence level.

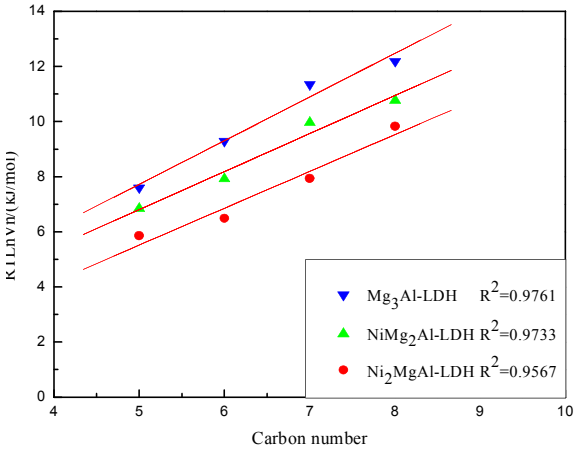

Fig. 1: Plot of $RT\ln V_N$ values versus carbon number for $Ni_xMg_{3-x}Al$-LDHs (x=0-2) to determine γ_s^d.

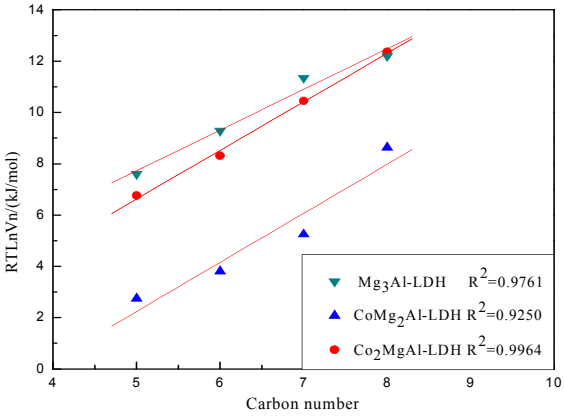

Fig. 2: Plot of $RT\ln V_N$ values versus carbon number for $Co_xMg_{3-x}Al$-LDHs (x=0-2) to determine γ_s^d.

According to Dorris and Gray theory, with the temperature of 423 K, the surface energy dispersive component of solid surface could be calculated by equation (4), and the results are listed in Table 2.

Table-2: γ_S^dvalues of $Ni_xMg_{3-x}Al$-LDHs and $Co_xMg_{3-x}Al$-LDHs (x=0-3).

LDHs	Mg_3Al	Mg_2NiAl	$MgNi_2Al$	Ni_3Al
γ_S^d(mJ·m^{-2})	48.02	36.49	26.31	13.58
LDHs	Mg_3Al	Mg_2CoAl	$MgCo_2Al$	Co_3Al
γ_S^d (mJ·m^{-2})	48.02	53.77	52.65	66.24

The γ_s^d can be used to assess the activity of the solid surface [16], the data in Table 2 suggests that with the increasing of Ni^{2+} in $Ni_xMg_{3-x}Al$-LDHs, γ_s^d showed a decreasing trend, and the surface activity decreased, while the stability generally enhanced. On the other side, with the increasing of Co^{2+} in $Co_xMg_{3-x}Al$-LDHs, γ_s^d showed a increasing trend, the surface activity increased, while the stability reduced.

This phenomenon was presumably due to the reason that Mg^{2+} was generally replaced by Co^{2+} through isomorphous substitution to form Co-O_2 octahedron, which increased the distortion degree of the system, leading the hydrogen bonding and electrostatic force between the subject and object decrease gradually, and the absolute value of the binding energy decreased, so the system stability decreased.

Analyzing the dispersive component of surface energy between $Ni_xMg_{3-x}Al$-LDHs and $Co_xMg_{3-x}Al$-LDHs, we found that the former were smaller, this may be due to the substitution of Ni^{2+}, the electron was transferred from the layer to the guest anion, which led to the enhancement of the supramolecular interaction and the binding energy of the system, result in $Ni_xMg_{3-x}Al$-LDHs appear more stable. The above conclusions were consistent with the results of relevant literature [13] and theoretical calculation results.

XRD analysis

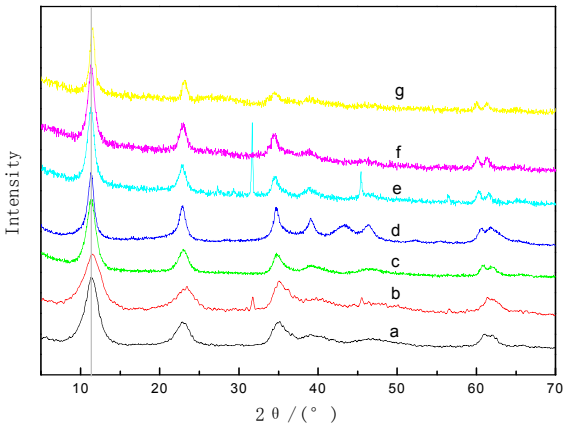

Fig. 3: XRD patterns of a-Ni_3Al-LDHs, b-$MgNi_2Al$-LDHs, c-Mg_2NiAl-LDHs, d-Mg_3Al-LDHs, e-Mg_2CoAl-LDHs, f-$MgCo_2Al$-LDHs, g-Co_3Al-LDHs.

As shown in Fig.3, the crystal sharp of the hydrotalcites were relatively single, and the characteristic diffraction peaks were close to each other, judging that the layer spacing was similar. The ionic radius of Ni^{2+} and Co^{2+} are 0.0690 nm and 0.0745 nm, which are similar to Mg^{2+} (0.0720 nm), having little effect on the structure of hydrotalcite, but still presented certain regularity. Compared with Ni^{2+} and Co^{2+} samples' layer spacing, we found that with the increasing of the incoming element on the plate, layer spacing changed slightly. In $Co_xMg_{3-x}Al$-LDHs system, with more and more Co^{2+} supersede Mg^{2+} by isomorphous substitution, layer spacing decreased to a certain extent，one each for 0.7887 nm, 0.7813 nm and 0.7708 nm. While spacing changes in $Ni_xMg_{3-x}Al$-LDHs showed the similar trends, which was consistent with the trend of lattice constants a and c.

The theoretical simulation results showed that with the introducing of Ni^{2+}, the valence electron configuration of metalions changed, while the plate structure did not cause serious distortion, and each M-O bond length decreased gradually, the average bond length gradually reduced from 0.2045 nm (Mg_3Al-LDHs) to 0.1986 nm ($Ni_xMg_{3-x}Al$-LDHs). According to crystal field theory, the interaction between the central ion and the ligand was called electrostatic effect, for the valence electron of the central metal atom passed out, led to the decreasing of the electron repulsion between the central ion and the ligand. Therefore, the coordination bond would be stronger,

resulting in a more stable octahedron, so the metal ion distance between the plate reduced gradually.

The same theoretical simulation method was also suitable for $Co_xMg_{3-x}Al$-LDHs, the conclusion of the two systems were consistent with the results obtained from the IGC test.

FT-IR analysis

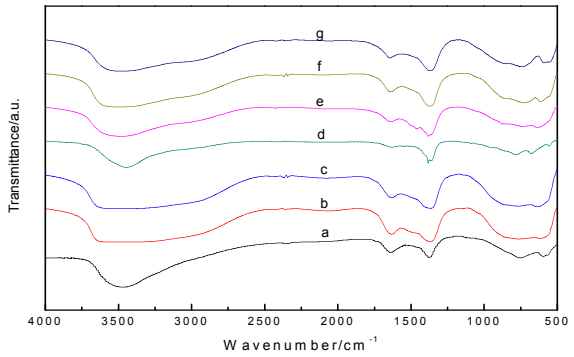

Fig. 4: FTIR spectra of a-Ni_3Al-LDHs, b-$MgNi_2Al$-LDHs c- Mg_2NiAl-LDHs, d-Mg_3Al-LDHs, e-Mg_2CoAl-LDHs, f-$MgCo_2Al$-LDHs, g-Co_3Al-LDHs.

The FTIR spectra of the seven samples at absorption peak of 3443-3496 cm $^{-1}$ are shown in Fig.4. The stretching vibrations between the layer board hydroxyl and interlayer water molecules, compared with hydroxyl free radical (3600 cm-1), mainly composed them, the peaks moved to low wave number, indicating that strong hydrogen bonding existed between interlayer water and layer board hydroxyl or carbonate. The vibration peaks in Fig.4 are listed in Table 3.

Table-3: FTIR data of $Ni_xMg_{3-x}Al$-LDHs and $Co_xMg_{3-x}Al$-LDHs(x=0-3).

System	a	b	c	d
Ni_3Al-LDHs	3478	1640	1380	415
$MgNi_2Al$-LDHs	3485	1633	1367	422
Mg_2NiAl-LDHs	3478	1631	1367	436
Mg_3Al-LDHs	3451	1629	1382	441
Mg_2CoAl-LDHs	3489	1636	1373	422
$MgCo_2Al$-LDHs	3496	1642	1373	428
Co_3Al-LDHs	3481	1650	1373	436

a. Stretching vibrations between layer board hydroxyl and interlayer water, b. H_2O bending vibration, c. CO_3^{2-} Symmetric vibration, d. M-O-M vibration

As a certain amount of water inserted into the surface adsorbed water and interlayer space of hydrotalcite, a bending vibration peak of crystalline water rise in the 1629-1650 cm^{-1}。

Compared the vibration of the interlayer CO_3^{2-} position at 1367-1382 cm^{-1} with the free state CO_3^{2-} (1430 cm^{-1}), the former moved to low wave number, demonstrating that hydrogen bonding existed in interlayer CO_3^{2-} and interlayer water molecules. With the increasing of Ni^{2+} and Co^{2+}, interlayer CO_3^{2-} remains substantially unchanged, meaning that the chemical environment in which it existed still unchanged significantly.

Computational methods and results

Combining the FTIR data in Table 3 and Mulliken bond population analysis in Table 4, we found that with the increasing of Ni^{2+} in $Ni_nMg_{3-n}Al$-LDHs, metal oxygen bond vibration peak moved to low wave number slightly. It was due to the increasing of Ni^{2+} in $Ni_nMg_{3-n}Al$-LDHs changed the M-O bond in the laminate from covalent to ionic gradually, indicating the covalent bonds decreased in the isomorphous substitution process, while the ionic bonds increased. Thus, the whole system changed from the covalent crystals to the ionic crystal gradually, and electrostatic interaction increase.

Table-4: Mulliken bond population (*e*) of $Ni_nMg_{3-n}Al$-LDHs (n=0-3).

System	Al-O	Mg-O	Ni-O	H-O
I	0.398	-0.723	——	0.575
II	0.370	-0.784	0.275	0.570
III	0.351	-0.857	0.242	0.578
IV	0.318	——	0.203	0.575

Combined the data analysis in table 3 and table 5, with the increasing of Co^{2+} in $Co_xMg_{3-x}Al$-LDHs, metal oxygen bond vibration peak moved to high wave number slightly, because the theoretical charge population of Al was 1.370-1.660 *e*, while Mg was 1.680-2.010 *e* and Co was 0.586-0.860 *e*. It was evident that the electrostatic force between metal cations and other anions was in order of $Mg^{2+} > Al^{3+} > Co^{2+}$. Thus, the energy of the sample decreased with the increasing of Co^{2+}, and finally moved to high wave number.

Table-5: Mulliken atomic population (*e*) of $Co_nMg_{3-n}Al$-LDHs (n=0-3).

System	Al	Mg	Co	Layer
I	1.420	1.668	——	0.64
II	1.510	1.810	0.586	0.67
III	1.580	1.970	0.705	0.69
IV	1.700	——	0.860	0.72

Conclusion

In summary, $Ni_xMg_{3-x}Al$-LDHs and $Co_xMg_{3-x}Al$-LDHs (x=0-3) with catalytic activity were synthesized through a co-precipitation method, all were characterized by IGC, X-ray diffraction and FT-IR, and get the results as follows: with the increase of Ni^{2+} in $Ni_xMg_{3-x}Al$-LDHs, the surface free energy decreased, and the stability increased, which were consistent with the computer simulated results. While, with the increase of Co^{2+}, the surface energy dispersive component increased, and the stability decreased. The adsorption capacity of $Co_xMg_{3-x}Al$-LDHs were larger than $Ni_xMg_{3-x}Al$-LDHs if the x were equal.

The γ_s^d values of $Co_xMg_{3-x}Al$-LDHs were larger than $Ni_xMg_{3-x}Al$-LDHs, indicating that LDHs with Co^{2+} possess had more powerful surface activities, and LDHs with Ni^{2+} showed higher stability than $Co_xMg_{3-x}Al$-LDHs and Mg_3Al-LDHs.

Acknowledgements

The authors thank The Public Welfare Analysis of Science and Technology Plan Projects of Zhejiang Province (2015C37034)

References

1. S. Kannan, Catalytic applications of hydrotalcite-like materials and their derived forms, *Catal. Surv. Asia*., **10**, 117 (2016).
2. A. Tsujimura, M. Uchida and A. Okuwaki, Synthesis and sulfate ion-exchange properties of a hydrotalcite-like compound intercalated by chloride ions, *J. Hazard. Mater.,* **143**, 582 (2007).
3. A. Valleta, M. Bessonb, G. Ovejeroa and J. García, Treatment of a non-azo dye aqueous solution by CWAO in continuous reactor using a Ni catalyst derived from hydrotalcite-like precursor, *J. Hazard. Mater*., **227**, 410 (2012).
4. M. Muñoz, S. Moreno and R. Molina, Synthesis of Ce and Pr-promoted Ni and Co catalysts from hydrotalcite type precursors by reconstruction method, *Int. J. Hydrogen.,* **37**, 18827 (2012).
5. Y. Zhao, Q. Z. Jiao, J. Liang and C. H. Li, Synthesis of Ni/Mg/Al Layered Double Hydroxides and Their Use as Catalyst Precursors in the Preparation of Carbon Nanotubes, *Chem. Res. Chinese U.,* **21**, 471 (2005).
6. B. H. Liu, H. L. Zhang and J. Y. Shen, Synthesis, Characterization and Isopropanol Catalytic Reaction of Mg/Al, Co /Al and Co/Mg/Al Mixed Oxides from Hydrotalcite and Hydrotalcite-like Precursors, Chinese *J. Inorg. Chem*., **21**, 43 (2005).
7. N. Q. Zhao, Master. Thesis, Preparation and catalysis studies of LDH grafted on carbon nanotubes and electrospinning study of PVP/LDH composite fibers, Beijing University of Chemical Technology, (2008).
8. G. S. Dritsas, K. Karatasos, C. Panayiotou. Investigation of thermodynamic properties of hyperbranched aliphatic polyesters by inverse gas chromatography, *J. Chromatogr. A*., **1216**, 8979 (2009).
9. N. E. Thaher and P. Choi, Effect of Preheating Treatment on the Measured Heats of Adsorption of Organic Probes on Clays with Different Surface Compositions, *Ind Eng Chem Res*., **51**, 7022 (2012).
10. J. M. Chen, N. Yan, Hydrophobization of bleached softwood kraft fibers via adsorption of organo-nanoclay *Bioresources*., **7**, 4132 (2012).
11. F. Zhang, X. X. Cao and Z. M. Ni, Surface Properties of Mg/Al-Hydrotalcite-like Compound and Its Modified Products, *Chinese J. Inorg. Chem*., **25**, 271 (2009).
12. X. W. Fu, Z. M. Ni and J. Liu, Surface Characterization of Copper-Aluminum-Magnesium Hydrotalcites Investigated by Inverse Gas Chromatography, *Acta Chim. Sinica*., **70**, 968 (2012).
13. Z. M. Ni, Y. LI, W. Shi, J. L. Xue and J. Liu, Supramolecular Structure, Electronic Property and Stability of Ni-Mg-Al Layered Double Hydroxides, *Acta Phys-Chim. Sin*., **28**, 2051 (2012).
14. M. Rückriema, A. Inayatb, D. Enkec, R. Gläserc, W. D. Einickec and R. Rockmann, Inverse gas chromatography for determining the dispersive surface energy of porous silica, *Colloid Surface A*., **357**, 21 (2010).
15. A. Askın and D. T. Yazici, Surface Characterization of Sepiolite by Inverse Gas Chromatography, Chromatographia., **61**, 625 (2005).
16. A. Voelkel, B. Strzemiecka, K. Adamska, K. Milczewska, Inverse gas chromatography as a source of physiochemical data, *J. Chromatogr. A*., **1216**, 1551 (2009).
17. S. K. Yun and T. J. Pinnavaia, Water Content and Particle Texture of Synthetic Hydrotalcite-like Layered Double Hydroxides, *Chem. Mat*., **7**, 348 (1995).